Table of Contents

CHAPTER 1

INFERRING SPECIES INTERACTIONS

1.1 Motivation

In this chapter we investiagte the possibility of quantifying species interaction strengths from observed population dynamics. This was discussed at length in the introduction (section **??**), however we now reiterate some of the important points here and to motivate our approach to the problem.

Inter-specific interactions are one of the major mechanisms that drive ecological processes. For example trophic interactions (e.g. predator-prey) define the pathways along which energy flows through an ecological community [REF], and are responsible for both top-down and bottom-up regulation of species abundances [REF]. Similary mutualistic and competitive interactions play an important role in shaping communities [REF]. However in nature the are many other mechanisms at work, such as seasonality. This, coupled with the difficulty in obtaining high resolution empirical data ahve made it very challenging to quantify the importantce of species interactions in generating observed spatila and temporal patterns in species abundances.

Take for example the classic hare-lynx dataset from Hudson Bay, Cananda [REF]. In this data the measured abundance of hare and lynx show oscillations..long thought to be predator-prey cycles (talk about ODEs and LV).. however dispted..quality of data..new phenomena showing seasonality..

We turn the question around..simulated systems for which we know species interactions and know they are responsible for the dyanimcs. We then try to qunatify the strength of these interactions by observing the dynamics..as such it is a step towards

The modelling approach in the previous chapters was *individual based*. Therefore in our simulations the interactions occured between individuals of a given species, as they do in nature. However the possibility for two individuals to interact was determined by the species interaction

network - if a link between two species exists in the network then individuals belonging to those species may interact.

.... Difficulty of relating species

Lacking suitable data - for which time-series and interaction (strengths) known..

Focus in predaot-rprey interactions..can be extended..

In this chapter we investiagte one novel method for inferring species interaction strengths...

Outline exactly what we will do e.g. two species focus, prey-dependenance

The general goal is to quantify inter-specific interaction strengths from observed population dynamics. As discussed, we currenlty lack suitable empircal data to do this (section 1.1). Therefore we develop a methodolgy using *simulated* population dynamcis. In the future this method could be applied to empircal abudnance time-series (see discussion in section 1.6). The population models used for simulation are, for the most part, standard ordinary differential equation (ODE) models. These are outlined in section 1.2.1. However we also present a preliminary application of our methdology to dynamics generated using the individual-based model from the previous chapters (section 1.5). To quantify the interaction strengths between species from their simulated dynamics we adapt a method from [1]. In short the method is used to fit a generalised Lotka-Volterra (GLV) model to the dynamics, giving numerical estimates of the interaction terms. The method is detailed in section 1.2.4 and the use of the GLV model to quantify interaction strengths is justified in section 1.2.3.

1.2 Methodology

We test a numerical method for estimating species interaction strengths from population dynamics. The method, described in section 1.2.4, works by fitting a generalised Lotka-Volterra model (GLV) to discrete observations of the dynamics. Therefore we obtain estimates of the 'best fit' GLV parameters, given the observed dynamics. These parameters include intrinsic growth rate coefficients for each species, and constant coefficients defining the strength of coupling between all species in the system (see section 1.2.3).

We test the method on two species predator-prey dynamics, which are simulated using ODE models. A general framework for the ODE modelling is given in section 1.2.1, from which we derive two distinct models.

1.2.1 Population models

To simulate population dynamics we use coupled ordinary differential equation (ODE) models. Although we focus on dynamics generated by predator-prey interactions, the ODE modelling framework may be adapted to model other types of interaction (e.g. mutulaism, competition). ODE models have been used extensively to simulate predator-prey dynamics at the species level [REFS]. They have several limitations in their usefullness. which are discussed in 1.6. However

they are a suitable choice for us becuse the equations explictly contain a term that defines the interactions between species. Therefore we are able to simulate populations dynamics for which we know the analytic form of all inter-specific interactions involved. This is the key to being able to test our method for quantifying interaction strengths [SECTION?].

We foucs on two-species systems. However the modelling framework, and the methodology in general may be extended to larger systems (see section 1.5). The growth rate for each species is defined by an ODE, which takes the general form:

$$\frac{dx_i}{dt} = G_i(x_i) + \Sigma_{j=1}^{N} F_{ij}(x_i, x_j) + \xi_i, \tag{1.1}$$

where x_i is the population density of species i; N is the number of species; G_i is the intrinsic growth function of species i; F_{ij} is a functional coupling between species i and j; and ξ_i is an additive noise term (see below).

We now restrict the discussion to two species systems. However all that follows may be extended to larger systems with little modification. This possibility is discussed in section 1.6[1]. Writing equation 1.1 for both species, and expanding the coupling function F_{ij} in terms of the *functional response*, we can express the entire system as:

$$\begin{aligned} \frac{dx_0}{dt} &= G_0(x_0) + a_{01}x_1H(x_0,x_1) + \xi_0, \\ \frac{dx_1}{dt} &= G_1(x_1) + a_{10}x_1H(x_0,x_1) + \xi_1 \end{aligned} \tag{1.2}$$

where species 0 is the prey; species 1 is the predator; the a_{ij} are constant coefficients and $H(x_0,x_1)$ is the functional reponse (FR) of the predator. The other symbols are the same as in equation 1.1. The FR gives the rate at which a single predator consumes prey i.e. the per-captia predation rate. Numerous functional forms have been proposed for the FR, and as we discussed the correct form is the subject of a long running debate [REFS]. However there are some widely used forms for both the FR and the intrinsic growth function G_i, which we adopt. We use the following intrinsic growth functions:

$$G_0(x_0) = r_0x_0\left(1 - \frac{x_0}{K_c}\right) \tag{1.3}$$

$$G_1(x_1) = -r_1x_1, \tag{1.4}$$

where $r_i \in \mathbf{R}^+$ is the intrinsic growth rate of species i and K_c is the carrying capacity of the prey species. Therefore the predator species has an exponential intrinsic mortality, as in the Lotka-Volterra equations [REFS], whereas the prey species has a saturating growth function, as in the Rosenzweig-MacArthur model [REF]. For the FR we focus mainly on those porposed by

[1] Or results presented in section...

Holling in the 1950s [REFs], which have been most widely used [REFS]. However other proposed forms of the FR are important in the debate and these are discussed in section 1.6. There are three Holling FRs, types I, II, and III which can be expressed as:

$$H_I(x_0,x_1) = x_0, \tag{1.5}$$

$$H_{II}(x_0,x_1) = \frac{x_0}{x_0+K_s}, \tag{1.6}$$

$$H_{III}(x_0,x_1) = \frac{x_0^2}{x_0^2+K_s^2}, \tag{1.7}$$

where x_0 is the prey densoty, and K_s is the saturation constant for the predator, giving the prey density at which the per-predator consumption rate reaches half-maximum. In the results presenetd in this chapter we use Holling types I and II for the simualtions. Therefore we have two dinstinct ODE models, which we will refer to as the *linear* and *holling* models. The linear model

These may be expressed in a reduced parameter space via substition as follows:...

$$\frac{d\chi_0}{dt} = A\chi_0(1-\chi_0) - B\chi_1 F(\chi_0,\chi_1) \tag{1.8}$$

$$\frac{d\chi_1}{dt} = -\chi_1 + C\chi_1 F(\chi_0,\chi_1), \tag{1.9}$$

where χ_1 is the predator density, χ_0 is the re-scaled prey density, $F(\chi_0,\chi_1)$ is the functional response (FR), and the parameters $A,B,C \in \mathbb{R}^+$. We use three different forms for the FR (see table 1.2) which gives three distinct simulation models.

The *linear* model:

$$\frac{d\chi_0}{dt} = A\chi_0(1-\chi_0) - B\chi_0\chi_1 \tag{1.10}$$

$$\frac{d\chi_1}{dt} = -\chi_1 + C\chi_0\chi_1, \tag{1.11}$$

The stationary points are given by:

$$\chi_0^* = \frac{1}{C} \tag{1.12}$$

$$\chi_1^* = \frac{A}{B}\left(1-\frac{1}{C}\right), \tag{1.13}$$

Therefore χ_0^* is always positive, and χ_1^* is positive if $c > 0$. ‘

The *holling* model:

	A	B	C	D
linear	0.1 - 100	0.1 - 100	1 - 100	N/A
holling	0.1 - 100	0.1 - 100	1.1 - 100	0.1-99

Table 1.1: Ranges from which parameters were selected unifomrly at random for the two ODE simulations models. The parameters are all allowed to vary over at least three orders of magnitude, to ensure that our investigation covers a large region of parameter space. The restrictions on parameters C and D ensure that for any value of one, it is possible to select the other so that the equilibirum population of both species is strictly positive.

$$\frac{d\chi_0}{dt} = A\chi_0(1-\chi_0) - \frac{B\chi_0\chi_1}{\chi_0+D} \tag{1.14}$$

$$\frac{d\chi_1}{dt} = -\chi_1 + \frac{C\chi_0\chi_1}{\chi_0+D}, \tag{1.15}$$

The stationary points are given by:

$$\chi_0^* = \frac{D}{C-1} \tag{1.16}$$

$$\chi_1^* = \frac{ACD(C-1-D)}{B(C-1)^2}, \tag{1.17}$$

Therefore χ_0^* is positive if $C > 1$, χ_1^* is positive if $C - D > 1$.

Additive noise term Discuss what it is, why and deterministic limit. Process error [REF]. We include additive noise ξ_i in some simulations (see section **??**). Therefore the (deterministic) population dynamics of a species is entirely determined by its intrinsic growth and interaction functions. SORT THIS OUT.

LOCAL STABILITY ANALYSIS..

1.2.2 Simulation procedure

We apply a strict recipe when running simulations in order to ensure consistency and to allow comparison of our numerical results. Consistency is ensured by the control of certain variables across simulations, and by our method for parameter selection. Parameters are selected uniformly at random from predefined ranges, which are given in table **??**.

This range ensures that a positive equilibrium is possible, but also allows for parameters to vary over at least three orders of magnitude so that our investigation covers a large region of parameter space.

such that the deterministic model ($\sigma_{noise} = 0$) has a positive equilibrium which is a stable spiral in the phase plane.

exhibit two full oscillations

An ensemble of 100 parameter sets were generated for each of the two ODE models. When expressed in reduced parameter space the *linear* model (equations 1.10,1.11) has three parameters (A,B,C), and the *holling* model (equations 1.14,1.15) has four (A,B,C,D).

Process error.

All simualtions were run using the first-order forward Euler method. Such that the ODE for each species dynamics is approximated by:

$$\chi_{i,t+1} = \chi_{i,t} + \Delta t \Delta\chi_{i,t} + \xi_{i,t}, \tag{1.18}$$

where Δt is the integration time step, $\Delta\chi_i$ is given by the right hand side of equations 1.8, 1.9; and $\xi_{i,t} \backsim \mathbb{N}(0, \sigma_{noise}\chi_{i,t}\Delta t)$ where σ_{noise} is the value quoted as noise intensity. In the event of stochastic extinction in either species, both population densities are reset to the initial conditions.

1.2.3 Interaction strength

Using the IM we can calculate the interaction strengths from our simualtion model.

There are numerous metrics available that can be used to quantify the strength of interactions between species. These other metrics are discussed in chapter **??** and in more detail in [REFS]. Of these metrics there is one that is a natural choice because we are able to make a direct comparison between the interaction strengths estimated from the population dynamics (using the method in section 1.2.4), and those evaluated from the simulation model (equations 1.1). This metric is called the *interaction matrix* (IM). The elements of the IM, α_{ij}, quantify the effect of a small change in the population density of species j on the per capita growth rate of species i. Therefore the IM elements are given by:

$$\alpha_{ij} = \frac{\partial}{\partial x_j}\left(\frac{1}{x_i}\frac{dx_i}{dt}\right), \tag{1.19}$$

where x_i and x_j are the population densities of species i and j respectively. In the case of our two species systems the IM is a 2×2 matrix, but trivially extends to quantify all pair-wise interactions between species in a N-species system. Since our simulation model has an explicit form for $\frac{dx_0}{dt}$ and $\frac{dx_1}{dt}$ we can evaluate the parital derivative in equation 1.19 to obtain analytic forms for all the IM elements (α_{00}, α_{01}, α_{10},α_{11}). That is, we can calculate the interaction strengths exactly from our simulation model.

However, as stated, our goal is quantify the interaction strengths using only the population dynamics. In order to do this we fit an ODE modle to the

1.2.4 Numerical estimation method

To estimate the inter-specific interaction strengths we use a numerical method to fit the GLV model to the population dynamics. The method gives 'best fit' estimates of the GLV parameters, which include constant coefficients for the interaction strengths.

We include here a derivation of the method, as published in [1], slightly adapted and simplified for our purposes. Say the system dynamics are governed by coupled differential equations of the form:

$$\dot{x_i} = \alpha_i f_i(x_i) + \Sigma_{j=1}^{N} J_{ij} g_{ij}(x_i, x_j), \tag{1.20}$$

where $\dot{x_i} = \frac{d}{dt}x_i$. The functions f_i and g_{ij} are *known*, so there are $N+1$ unknowns in equation 1.20 (α_i and $J_{i,j}$ for $j = 1,...,N$). Therefore, if we knew the exact values of $\dot{x_i}, x_i$ and the x_j's, at $N+1$ timepoints, then we could solve the equation for α_i and the $J_{i,j}$'s. In any practical application our knowledge of the system is not *exact*; the system is subject to noise; and the model is an imperfect description of the dynamics. So the equation cannot be solved exactly. We must look for an approximate solution.

The full state of the system is observed at time points t_m for $m \in 1,..,M,M+1$. These observations are used to construct estimates for the states and their time-derivatives, for every unit i.

The simplest way to estimate the time-derivatives is to take the finite difference between observations at two consecutive time points, such that

$$\hat{\dot{x}}_i(\tau_m) := \frac{x_i(t_m) - x_i(t_{m-1})}{t_m - t_{m-1}}, \tag{1.21}$$

where $\tau_m \in \mathbb{R}, m \in \{1,...,M\}$ is the midpoint of the two time-points:

$$\tau_m := \frac{t_{m-1} + t_m}{2}. \tag{1.22}$$

To evaluate the functions f_i, g_i at these new time-points we must estimate the states $x_i(\tau_m)$ from the observations. We use the simple linear interpolation

Response Type	$F(X_0, X_1)$	α_{01}	α_{10}
Linear	X_0	$-B$	C
Holling II	$\frac{X_0}{X_0+D}$	$\frac{-B}{X_0+D}$	$\frac{CD}{(X_0+D)^2}$

Table 1.2: Table showing the two types of functional response used, their expression in the reduced parameter space, and the corresponding interaction strengths (derived by applying expression **??** to equations 1.8,1.9).

$$\hat{x}_i(\tau_m) := \frac{x_i(t_{m-1}) + x_i(t_m)}{2}. \tag{1.23}$$

Then, from equation 1.20, we have M equations:

$$\dot{\hat{x}}_i(\tau_m) = \alpha_i f_i(\hat{x}_i(\tau_m)) + \Sigma_{j=1}^{N} J_{i,j} g_{ij}(\hat{x}_i(\tau_m), \hat{x}_j(\tau_m)). \tag{1.24}$$

We now simplify the notation such that equation 1.24 may be written

$$\dot{\hat{x}}_{i,m} = \alpha_i f_{i,m} + \Sigma_{j=1}^{N} J_{i,j} g_{i,j,m}, \tag{1.25}$$

Were the subscripts i, j indicate the unit, and m indicates the time-point for which the equation holds. This can be expressed in matrix form:

$$X_i = J_i G_i, \tag{1.26}$$

where we have

$$X_i = \begin{pmatrix} \dot{\hat{x}}_{i,1} & \dot{\hat{x}}_{i,2} & \cdots & \dot{\hat{x}}_{i,M} \end{pmatrix} \in \mathbb{R}^{1 \times M}, \tag{1.27}$$

$$J_i = \begin{pmatrix} \alpha_i & J_{i,1} & J_{i,2} & \cdots & J_{i,N} \end{pmatrix} \in \mathbb{R}^{1 \times (N+1)}, \tag{1.28}$$

$$G_i = \begin{pmatrix} f_{i,1} & f_{i,2} & \cdots & f_{i,M} \\ g_{i,1,1} & g_{i,1,2} & \cdots & g_{i,1,M} \\ g_{i,2,1} & g_{i,2,2} & \cdots & g_{i,2,M} \\ \vdots & \vdots & \ddots & \vdots \\ g_{i,N,1} & g_{i,N,2} & \cdots & g_{i,N,M} \end{pmatrix} \in \mathbb{R}^{(N+1) \times M}. \tag{1.29}$$

Here J_i is the ith row of the full coupling matrix J and represents the input coupling strengths to the unit i. Equation 1.26 has $N+1$ and M equations. In the case when $M > N+1$ the system is over constrained and there is no exact solution in general. We look for an approximate solution $\hat{J}_i$ that minimises the error between the LHS and RHS of equation 1.26. We take the error function:

$$E_i(\hat{J}_i) = \Sigma_{m=1}^{M} (X_{i,m} - \Sigma_{k=1}^{N} \hat{J}_{i,k} g_{i,k,m})^2, \tag{1.30}$$

which we want to minimise with respect to the matrix elements $\hat{J}_{i,k}$. That is

$$\frac{\partial}{\partial \hat{J}_{i,k}} E_i(\hat{J}_i) \stackrel{!}{=} 0. \tag{1.31}$$

By taking the derivative of the RHS of equation1.30 we have that:

$$\begin{aligned} \frac{\partial}{\partial \hat{J}_{i,k'}} E_i(\hat{J}_i) &= \frac{\partial}{\partial \hat{J}_{i,k}} [\Sigma_{m=1}^{M} (X_{i,m} - \Sigma_{k=1}^{N} \hat{J}_{i,k} g_{i,k,m})^2] \\ &= -2\Sigma_{m=1}^{M} (X_{i,m} - \Sigma_{k=1}^{N} \hat{J}_{i,k} g_{i,k,m}) g_{i,k',m} \end{aligned}$$

To find the minimum of the error function we equate this to zero, giving:

$$\begin{aligned} 0 &= \Sigma_{m=1}^{M} (-X_{i,m} g_{i,k',m} + g_{i,k',m} \Sigma_{k=1}^{N} \hat{J}_{i,k} g_{i,k,m}) \\ &= (-X_i G_i^T)_{k'} + \Sigma_{m=1}^{M} g_{i,k',m} (\hat{J}_i G_i)_m \\ &= (-X_i G_i^T)_{k'} + \Sigma_{m=1}^{M} (\hat{J}_i G_i)_m G_{i,m,k'}^T \\ &= -X_i G_i^T + \hat{J}_i G_i G_i^T \end{aligned} \tag{1.32}$$

Therefore we conclude that:

$$\hat{J}_i = X G_i^T (G_i G_i^T)^{-1}, \tag{1.33}$$

which, in our case, is the analytic form for the best estimate of the row corresponding to species i in parameter matrix of the GLV model.

1.2.5 Examples

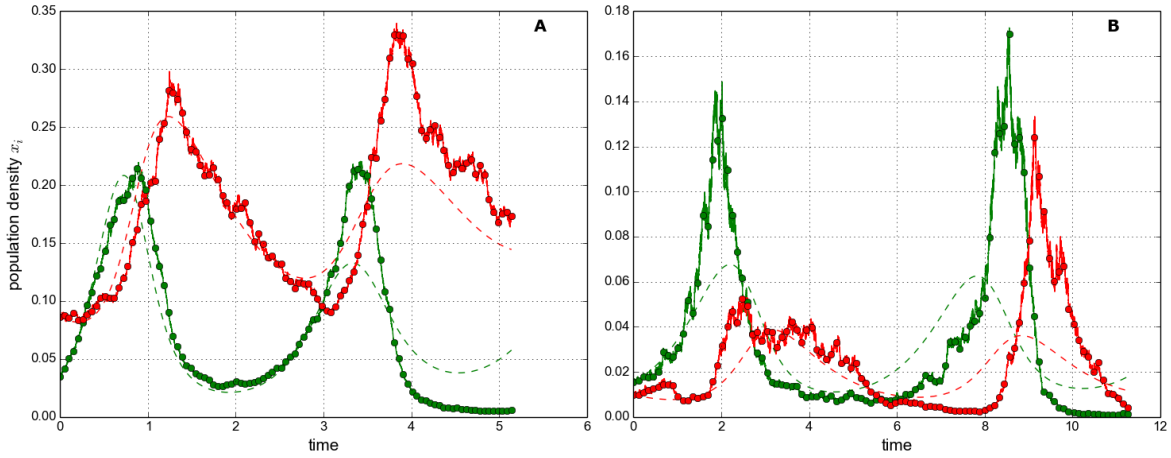

Figure 1.1: Example linear dynamics. 100 sampels. Two different parameter sets. A: noise=20. B:noise=50.

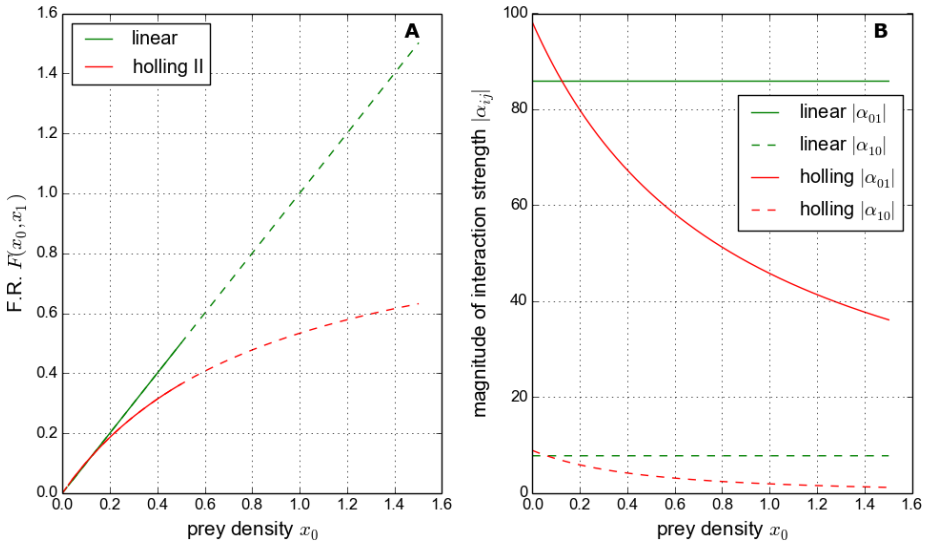

Figure 1.2: Example FR. Parameters?

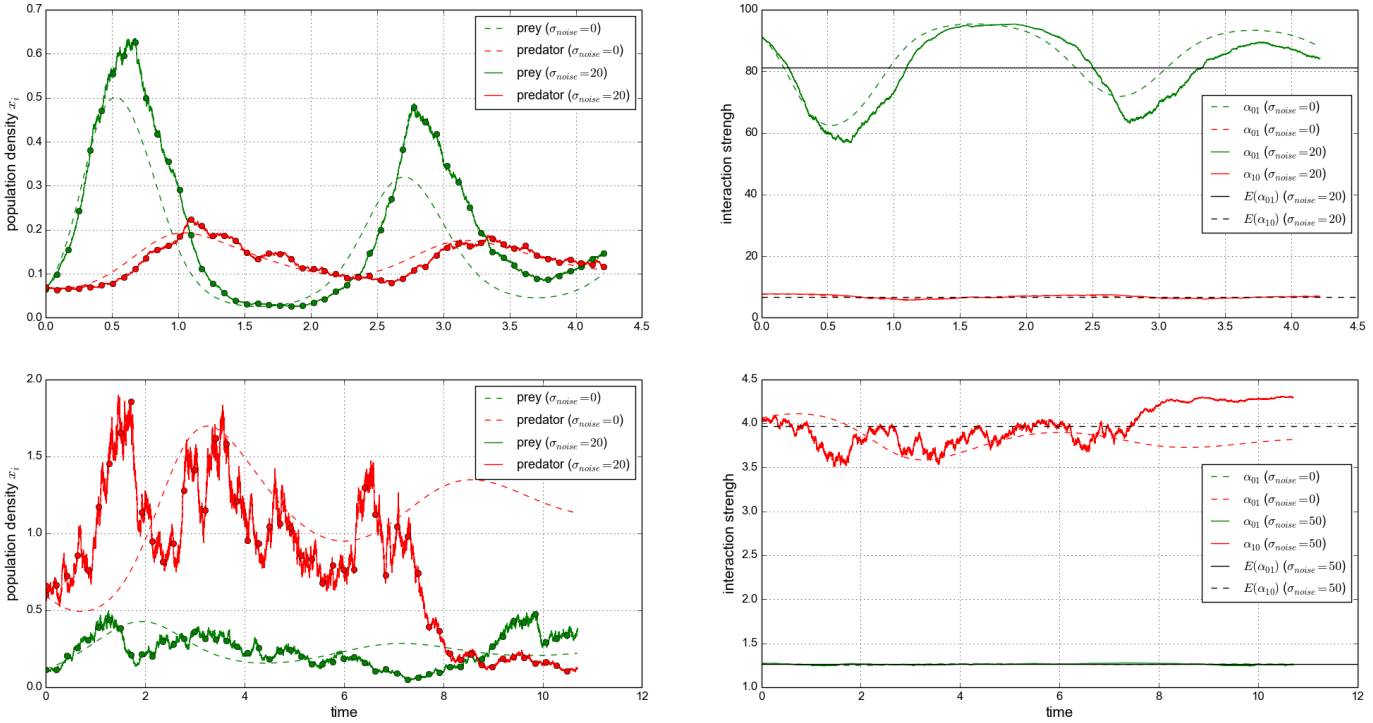

Figure 1.3: Example HOlling II dynamics.

1.3 Results

In this sections we characterise the numerical performance of the method, described in section 1.2.4, for estimating the strength of interactions between species. The method is tested on the dynamics of two different ODE systems: a Lotka-Volterra (LV) and a Holling type II (HII) system. In the first case it is simply a test of a model fitting procedure. This is because the method works by fitting a generalised Lotka-Volterra (GLV) model to the dynamics, and he LV systems can be expressed as a GLV systems. Therefore we are simply simulating using one model, and then testing a method of estimating the model parameters form the simulated dynamics. We test the effects of noise and sampling frequency. In the second case, the HII system cannot be expressed as a GLV system. Therefore the GLV model that we fit can only approximate the dynamics and we cannot make a direct comparison between the parameters of the simulation model and the GLV model used for estimation. In this case we comapre to the mean interaction strengths (see section 1.3.2.

1.3.1 Lotka-Volterra system

Initially we run repeated simulations of the LV model using a single parameter set. We investigate how the numerical estimates of the model parameters respond to two variables: the level of noise in the simulations; and the number of samples used for estimation. Other variables are held constant using the simulation procedure described in section 1.2.2. We then generalise these results by looking at the relative error in the estimates, for repeated simulations using an ensemble of 100 selected parameter sets (as described in section 1.2.2).

Single parameter set. Here we can make direct comparison between model parameters. The GLV model for two species has six parameters: $r_0, r_1, J_{00}, J_{01}, J_{10}, J_{11}$. These correspond respectively to the following constant values of the LV system used for simulations: $A, -1, -A, -B, C, 0$ (see equation **??**). In general we find that the numerical estimates perform well at low noise intensities and poorly at high noise intensities. This is illustrated in figures 1.4 and 1.5. We also find that the estimates improve with the number of samples used, up to a point. Beyond this point the use of more samples does little to improve to estimates, and in some cases makes them worse. This behaviour is illustrated in figures 1.6 and 1.7. These patterns were found to hold across all parameter sets investiagted, but are only shown using a single parameter set here for clarity.

In panel **A** of figures 1.4 and 1.5 we see that the mean value of the estimates approaches the true value for low noise and, in panel **B** that the variance in the estimates approaches zero. This tells us that the method consistently gives a good fit of the GLV to the dynamics of the LV system, even when only 100 sample points are used (figure 1.4). As the noise intesitiy is increased the mean values of the estimates deviate from the true values, and the standard deviation in the estimates increases. Comparing the two figures we see that the response to noise is very similar

whether 100 or 10,000 samples are used. A notable exception to this is a spike in the variance in panel **B** of figure. However this appears to be a single statistically anomolous result and not part of the trend. Panel **C** of both figures shows that the error function, which is minimised by the estimation method, increases with noise for both species. This cannot be directly compared between the two plots because of the different number of samples used. However it indicates that in both cases (100 and 10,000 samples) the quality of the fit is high in the deterministic case, and decreases with noise.

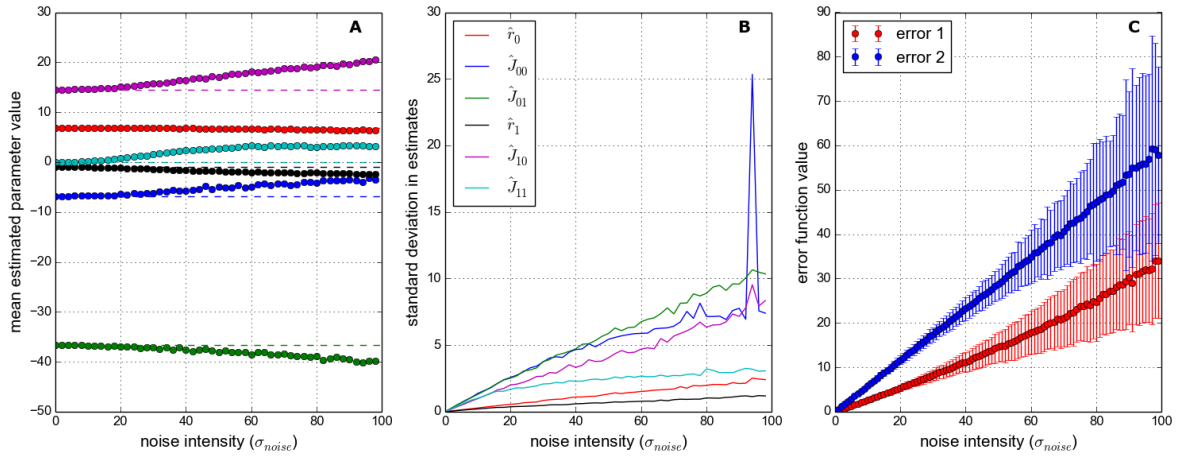

Figure 1.4: Effect of noise on numerical estimates. Here the method uses 100 samples from simulated dynamics. All simulations run using the LV model with a single parameter set. The noise intensity varies between 0 (deterministic) and 100. See section 1.2.5 for an intuition of how noisy this is. 1000 repeat smulations run at each noise level. **Panel A**: Mean estimated parameter values (each dot representing mean over 1000 repeats). The 'true' paramter values of the simulation model are shown by dashed lines. **Panel B:** Standard deviation in estimates. **Panel C:** Value of the error functions used in the estimation method, one for each species. The dots show the mean error, and the bars show ± one standard deviation.

We now look at how the estimates respond to the number of samples used, in the cases of low and high noise intensity. Figure 1.6 shows the low noise case, with $\sigma_{noise} = 10$. In panel **A** we see that the mean value of the estimates quickly converges to close to the true parameter values, as the number of samples increases. Panel **B** shows that the standard deviation in the estimates quickly becomes small, but non-zero. Above about 32 samples there is no visible improvement in the estimates, as measured by the mean or standard deviation. In figure 1.7 we see the effect of a higher noise intensity. Here we have $\sigma_{noise} = 50$. Panel **A** shows that the estimates do not converge on the true parameter values, even for large numbers of samples. Also the standard deviation in the estimates, shown in panel **B**, is higher than in the low noise case. Again we find that there is little, if any, improvement in the estimates beyond about 32 samples.

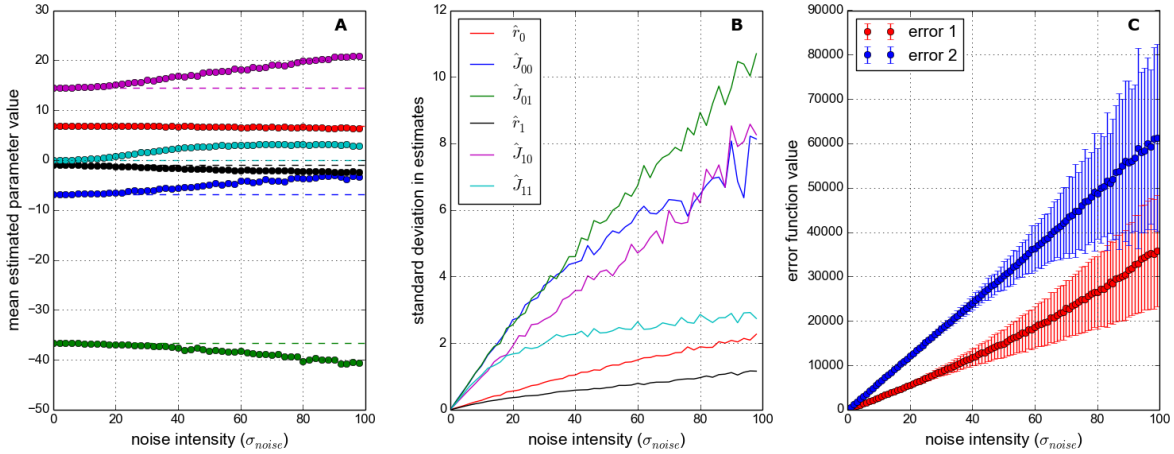

Figure 1.5: Exactly as in figure 1.4 but using 10,000 samples from the simulated dynamics.

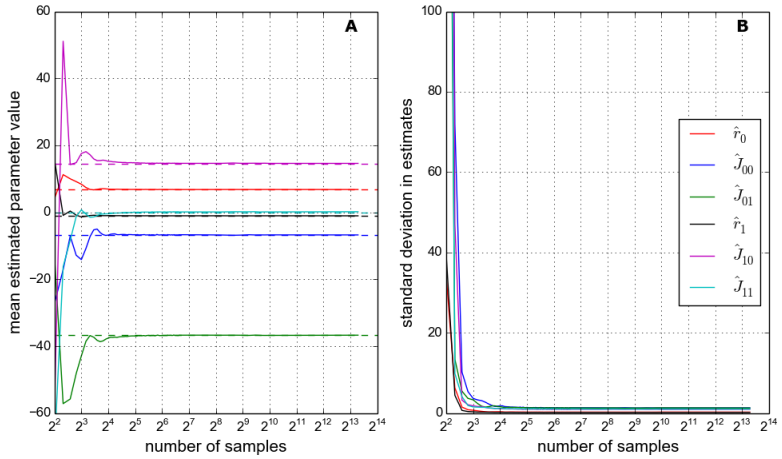

Figure 1.6: Effect of the number of samples on numerical estimates. All simulations run using the LV model with a single parameter set. The noise intensity $\sigma_{noise} = 10$. Number of samples ranges from 4 to 10,000. Samples drawn from simulated dynamics at equal intervals. 1000 repeat smulations for each number of samples. **Panel A**: Solid lines show mean estimated parameter values. Dashed lines show the 'true' paramter values of the simulation model. **Panel B:** Standard deviation in estimates.

Ensemble of parameter sets. Run 10 repeats for each of 100 parameter sets. In general the trends described above hold across the ensemble..

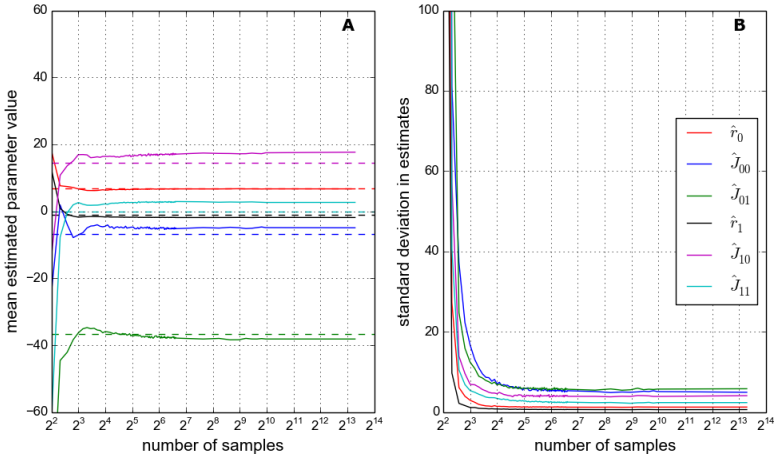

Figure 1.7: Exactly as in figure 1.6 but with noise intesity $\sigma_{noise} = 50$.

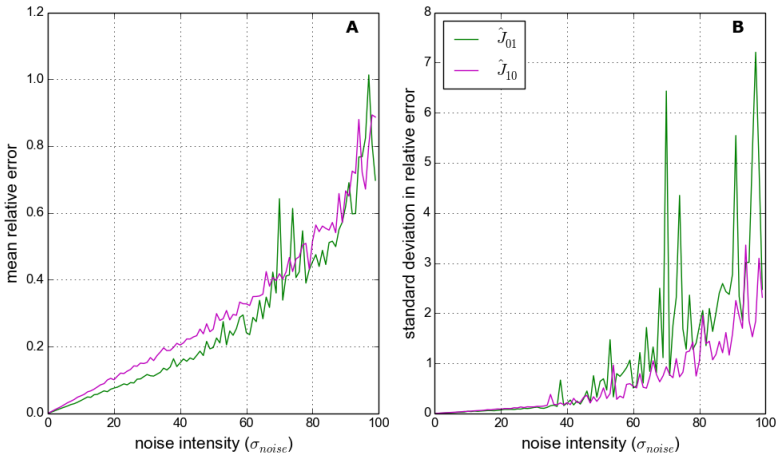

Figure 1.8: Nonsense. 1000 samples used.

1.3.2 Holling system

1.3.3 Range sampling

1.4 TEMP : other results

This section shows some plots which I was not planning to put into the thesis but are worth discussing..

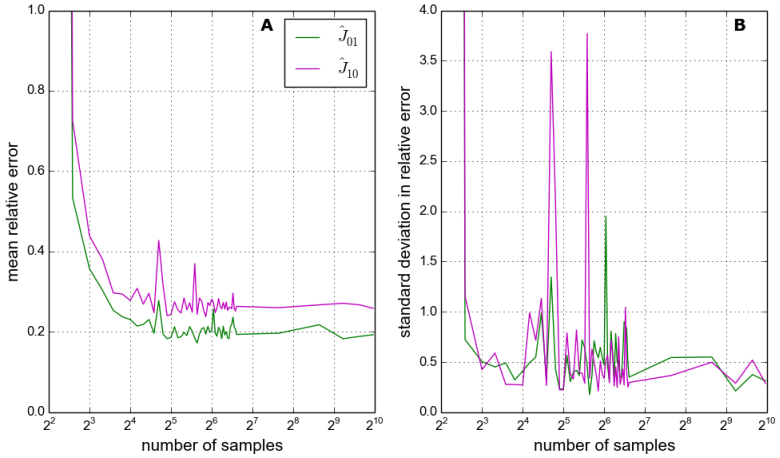

Figure 1.9: Nonsense. Noise is 50.

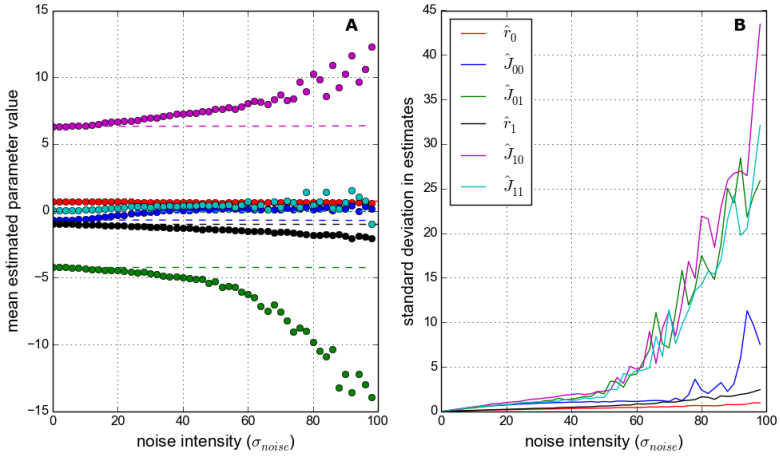

Figure 1.10: Nsamples is 10,000.

1.5 Application to IBM (optional)

1.5.1 Testing functionl response

1.5.2 Extend methodology (3 and 4 species)

1.5.3 Results

1.6 Discussion

Points referenced in text above, make sure to discuss them!..

- Discuss how this methodology could be used on empircal data...

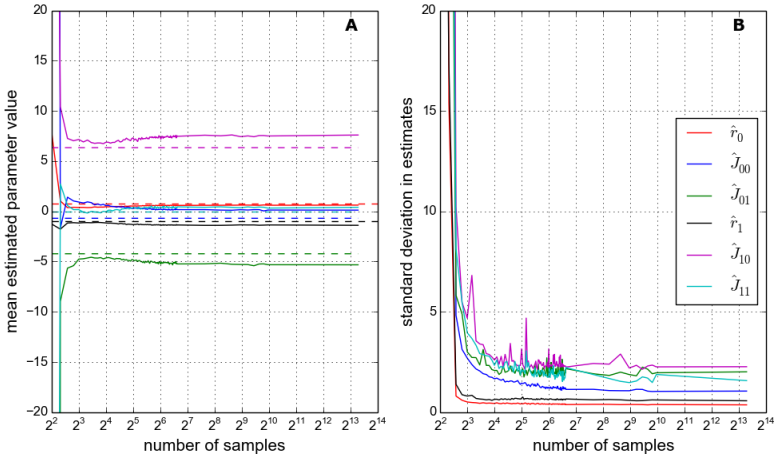

Figure 1.11: Noise is 50.

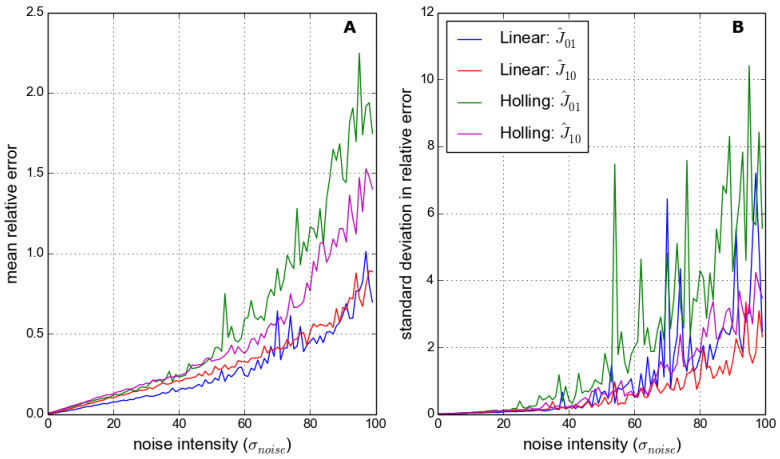

Figure 1.12: Noise is 50.

- Limitations of ODE models (non-spatial, repsonse to debate on FR)
- Possibility of extending to more than two specie systems (if this is actually done then change ref in text above)
- discussion of other forms of FR (not H) - or disucssed already in inro?
- good GLV fit to LV even with 100 sample points - realistic?

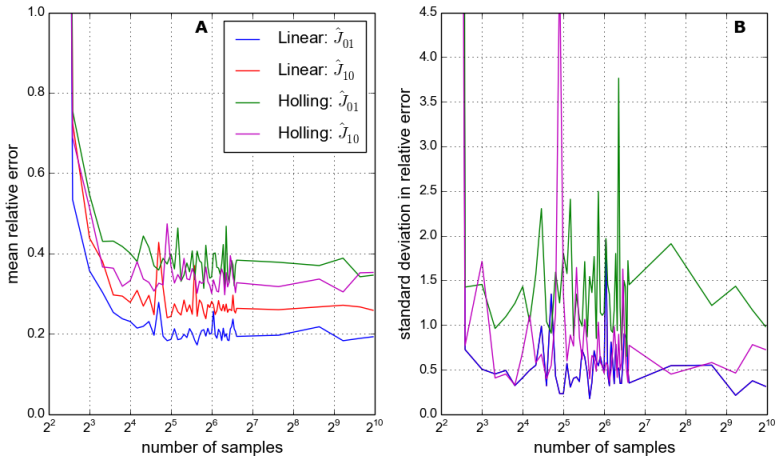

Figure 1.13: Noise is 50.

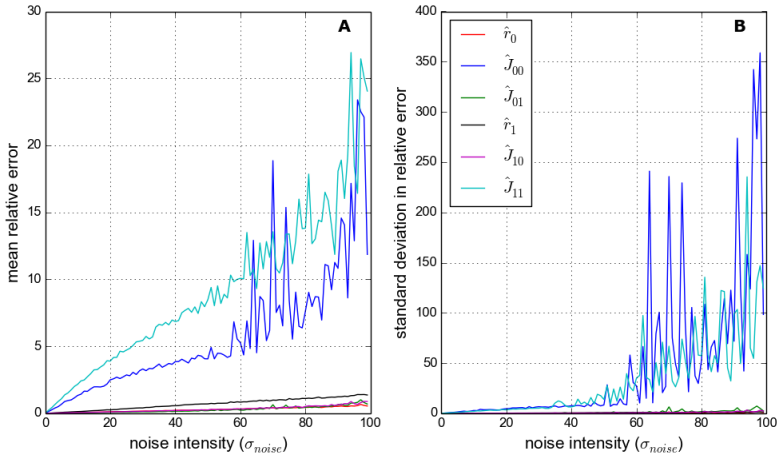

Figure 1.14: Nonsense. 1000 samples used.

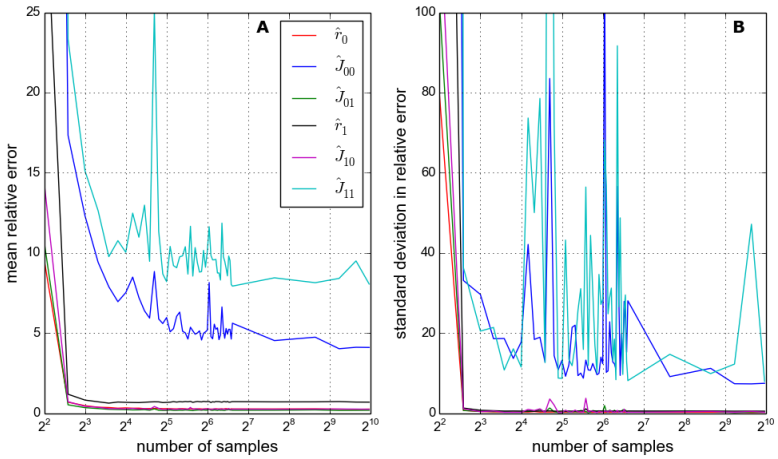

Figure 1.15: Nonsense. Noise is 50.

BIBLIOGRAPHY

[1] S. G. SHANDILYA AND M. TIMME, *Inferring network topology from complex dynamics*, New Journal of Physics, 13 (2011), p. 013004.